

Spin Canting and Slow Relaxation in a 3D Pillared Nickel–Organic Framework

Fu-Ping Huang, Jin-Lei Tian,* Dong-Dong Li, Gong-Jun Chen, Wen Gu, Shi-Ping Yan,* Xin Liu, Dai-Zheng Liao, and Peng Cheng

Department of Chemistry, Nankai University, Tianjin 300071, People's Republic of China

Received December 8, 2009

A 3D nickel–organic framework formulated as $\{[\text{Ni}_2(\text{fum})_2(\text{bpt})_2(\text{H}_2\text{O})] \cdot 3\text{H}_2\text{O}\}_n$ (**1**), built from a mixed fumaric ion (fum), 1*H*-3,5-bis(4-pyridyl)-1,2,4-triazole (bpt), and nickel salt, has been hydrothermally synthesized and characterized. Compound **1**, having a Ni–fum chain structure in which the chains are pillared by the bpt spacers in a 3D “brick-wall”-like architecture, exhibits canted antiferromagnetism at 5.0 K. Below this temperature, slow relaxation is observed from the alternating-current susceptibility measurements corresponding to the spin-glass-like behavior.

Introduction

In the field of molecule-based magnetism, tremendous effort has been devoted to the design of magnetic materials that exhibit spontaneous magnetization.¹ Generally, two approaches, ferro- and ferrimagnetic (FO and FI), can lead to spontaneous magnetization. Because of the parallel alignment of the moments, the ferromagnets naturally have high spontaneous magnetization.² However, because of the infrequency and weakness of the FO interaction compared to the antiferromagnetic (AF) interaction, ferromagnets were somewhat limited and more attention has been paid to the FI systems. The FI approach was first realized by Neél, the 1970 Nobel Laureate in Physics, in his famous studies of garnets and spinel ferrites and then developed by Kahn, Verdager,

and co-workers.³ In the AF systems, the weak ferromagnets due to spin canting also have spontaneous magnetization and are efficient in constructing molecular magnets.^{4–6} It is well-known that spin canting can arise from two contributions: (1) the presence of an antisymmetric exchange and (2) the existence of single-ion magnetic anisotropy.⁷ With respect to spin centers, the canted systems including Fe^{II}, Co^{II}, and Mn^{III} with large anisotropy have been widely characterized and magnetically investigated.^{5d,8,9} Despite the fact that Ni^{II} is known to display large single-ion anisotropy,¹⁰ to date only a handful of Ni^{II} complexes display spin-canted behavior; particularly rare are those showing the coexistence of spin canting and spin-glass (SG) behavior.¹¹ The SG behavior constitutes an illustrative manifestation of

*To whom correspondence should be addressed. E-mail: (J.-L.T.), yansp@nankai.edu.cn (S.-P.Y.). Tel.: +86-022-23505063. Fax: +86-022-23502779.

(1) (a) Larionova, J.; Kahn, O.; Golhen, S.; Ouahab, L.; Clérac, R. *J. Am. Chem. Soc.* **1999**, *121*, 3349. (b) Miller, J. S. *Adv. Mater.* **2002**, *14*, 1105. (c) Galán-Mascarós, J. R.; Dunbar, K. R. *Angew. Chem.* **2003**, *115*, 2391. *Angew. Chem., Int. Ed.* **2003**, *42*, 2289. (d) *Magnetism: Molecules to Materials*; Miller, J. S., Drillon, M., Eds.; Wiley-VCH: New York, 2002–2005; Vols. I–IV.

(2) (a) Goodenough, J. B.; Loeb, A. L. *Phys. Rev.* **1955**, *98*, 391. (b) Goodenough, J. B. *Phys. Rev.* **1956**, *100*, 564. (c) McConnell, H. M. *J. Chem. Phys.* **1963**, *39*, 1910.

(3) (a) Kahn, O.; Pei, Y.; Verdager, M.; Renard, J. P.; Sletten, J. *J. Am. Chem. Soc.* **1988**, *110*, 782. (b) Holmes, M. S.; Girolami, G. S. *J. Am. Chem. Soc.* **1999**, *121*, 5593. (c) Manriquez, J. M.; Yee, G. T.; Mclean, R. S.; Epstein, A. J.; Miller, J. S. *Science* **1991**, *252*, 1415. (d) Ferlay, S.; Mallah, T.; Quahes, R.; Veillet, P.; Verdager, M. *Nature* **1995**, *378*, 701.

(4) (a) Carlin, R. L. *Magnetochemistry*; Springer-Verlag: Berlin, Germany, 1986. (b) Batten, S. R.; Murray, K. S. *Coord. Chem. Rev.* **2003**, *246*, 103. (c) Lappas, A.; Wills, A. S.; Prassides, K.; Kurmoo, M. *Phys. Rev. B* **2003**, *67*, 144406. (d) Kurmoo, M.; Kumagai, H.; Green, M. A.; Lovett, B. W.; Blundell, S. J.; Ardavan, A.; Singleton, J. *J. Solid State Chem.* **2001**, *159*, 343.

(5) (a) Wang, X.-Y.; Wang, L.; Wang, Z.-M.; Gao, S. *J. Am. Chem. Soc.* **2006**, *128*, 674. (b) Wang, X.-Y.; Wang, Z.-M.; Gao, S. *Inorg. Chem.* **2008**, *47*, 5720. (c) Zeng, M.-H.; Zhang, W.-X.; Sun, X.-Z.; Chen, X.-M. *Angew. Chem., Int. Ed.* **2005**, *44*, 3079. (d) Kurmoo, M. *Chem. Soc. Rev.*, **2009**, *38*, 1353 and references cited therein.

(6) (a) Rodríguez, A.; Kivekäs, R.; Colacio, E. *Chem. Commun.* **2005**, 5228. (b) Ouellette, W.; Prosvirin, A. V.; Chieffo, V.; Dunbar, K. R.; Hudson, B.; Zubieta, J. *Inorg. Chem.* **2006**, *45*, 9346. (c) Bernot, K.; Luzon, J.; Sessoli, R.; Vindigni, A.; Thion, J.; Richeter, S.; Leclercq, D.; Larionova, J.; van der Lee, A. *J. Am. Chem. Soc.* **2008**, *130*, 1619. (d) Pali, A. V.; Reu, O. S.; Ostrovsky, S. M.; Klodishner, S. I.; Tsukerblat, B. S.; Sun, Z.-M.; Mao, J.-G.; Prosvirin, A. V.; Zhao, H.-H.; Dunbar, K. R. *J. Am. Chem. Soc.* **2008**, *130*, 14729.

(7) (a) Manson, J. L.; Kmetz, C. R.; Palacio, F.; Epstein, A. J.; Miller, J. S. *Chem. Mater.* **2001**, *13*, 1068. (b) Jia, H.-P.; Li, W.; Ju, Z.-F.; Zhang, J. *Chem. Commun.* **2008**, 371.

(8) (a) Batten, S. R.; Murray, K. S. *Coord. Chem. Rev.* **2003**, *246*, 103. (b) Lappas, A.; Wills, A. S.; Prassides, K.; Kurmoo, M. *Phys. Rev. B* **2003**, *67*, 144406. (c) Feyerherm, R.; Loose, A.; Ishida, T.; Nogami, T.; Kreitlow, J.; Baabe, D.; Litterst, F. J.; Süllow, S.; Klaus, H. H.; Doll, K. *Phys. Rev. B* **2004**, *69*, 134427.

(9) (a) Mossin, S.; Weihe, H.; Sørensen, H. O.; Lima, N.; Sessoli, R. *Dalton Trans.* **2004**, 632. (b) Bernot, K.; Luzon, J.; Sessoli, R.; Vindigni, A.; Thion, J.; Richeter, S.; Leclercq, D.; Larionova, J.; van der Lee, A. *J. Am. Chem. Soc.* **2008**, *130*, 1619.

(10) (a) Rogez, G.; Rebilly, J. N.; Barra, A. L.; Sorace, L.; Blondin, G.; Kirchner, N.; Duran, M.; Van Slageren, J.; Parsons, S.; Ricard, L.; Marvilliers, A.; Mallah, T. *Angew. Chem., Int. Ed.* **2005**, *44*, 2. (b) Krzystek, J.; Park, J. H.; Meisel, M. W.; Hitchman, M. A.; Stratemeier, H.; Brunel, L. C.; Telsler, J. *Inorg. Chem.* **2002**, *41*, 4478.

(11) (a) Liu, X.-T.; Wang, X.-Y.; Zhang, W.-X.; Cui, P.; Gao, S. *Adv. Mater.* **2006**, *18*, 2852. (b) Cao, D.-K.; Li, Y.-Z.; Zheng, L.-M. *Inorg. Chem.* **2007**, *46*, 7571.

the slow relaxation phenomenon, which may have potential applications in categorization theory, information theory, associative memories, and combinatorial optimization.¹² The best known and most intensely studied SG phenomena are coined to describe some magnetic alloys or metal oxides depending on their particle size.¹³ Nonetheless, a few Ni^{II} complexes with SG behavior have been reported that mainly focused on low-dimensional single-molecule magnet (SMM)/single-chain magnet (SCM) systems¹⁴ and high-dimensional cyanide/oxalate-bridged systems.¹⁵

Herein, we report an interesting 3D pillared carboxylate-bridged Ni^{II} coordination polymer, $\{[\text{Ni}_2(\text{fum})_2(\text{bpt})_2(\text{H}_2\text{O})] \cdot 3\text{H}_2\text{O}\}_n$ **1**; H₂fum = fumaric acid, bpt = 1*H*-3,5-bis-(4-pyridyl)-1,2,4-triazole, which possesses an interesting 3D “brick-wall”-like network with a (3,5)-connected geometrical topology and shows the coexistence of weak ferromagnetism and slow relaxation behavior at low temperature.

Experimental Section

Materials and Physical Measurements. 1*H*-3,5-Bis(4-pyridyl)-1,2,4-triazole (bpt) was prepared according to the literature.¹⁶ All reagents were used as received without further purification. IR spectra were taken on a Perkin-Elmer Spectrum One FT-IR spectrometer in the 4000–400 cm⁻¹ region with KBr pellets. Elemental analyses for C, H, and N were carried out on a Perkin-Elmer model 2400 II elemental analyzer. Temperature- and field-dependent magnetic measurements were carried out on a SQUID-MPMS-XL-7 magnetometer. Diamagnetic corrections were made with Pascal's constants.

Synthesis of 1. A mixture of H₂fum (0.058 g, 0.5 mmol), Ni(NO₃)₂·6H₂O (0.145 g, 0.5 mmol), NaOH (0.040 g, 1 mmol), bpt (0.112 g, 0.5 mmol), triethylamine (0.1 mL), and H₂O (10 mL) was stirred in a Teflon-lined autoclave under autogenous pressure at 423 K for 4 days. Then red blocklike crystals of **1** were obtained and picked out, washed with distilled water, and dried in air. Yield: 35% (based on Ni^{II}). Elem. anal. Calcd for C₃₂H₃₀N₁₀Ni₂O₁₂: C, 44.48; H, 3.50; N, 16.21. Found: C, 44.69; H, 3.72; N, 16.48. IR (KBr): 3442s, 1617s, 1574s, 1513m, 1377s, 1217m, 1000m, 847w, 680s.

X-ray Crystallography. Diffraction data were collected on a Bruker Smart Apex CCD diffractometer with graphite-monochromated Mo K α radiation ($\lambda = 0.71073$ Å), and the absorp-

Table 1. Crystal Data and Structure Refinement for **1**

empirical formula	C ₃₂ H ₃₀ N ₁₀ Ni ₂ O ₁₂
fw	864.04
cryst syst	monoclinic
space group	<i>P</i> 2 ₁ / <i>c</i>
<i>a</i> (Å)	8.280(2)
<i>b</i> (Å)	28.059(6)
<i>c</i> (Å)	16.424(3)
β (deg)	94.02(3)
volume (Å ³)	3806.4(13)
<i>Z</i>	4
calcd density (Mg/m ³)	1.497
cryst size (mm ³)	0.23 × 0.12 × 0.08
indep reflns	6651
GOF on <i>F</i> ²	1.01 (<i>R</i> _{int} = 0.085)
final <i>R</i> indices [<i>I</i> > 2 σ (<i>I</i>)]	0.079
<i>R</i> indices (all data)	0.166

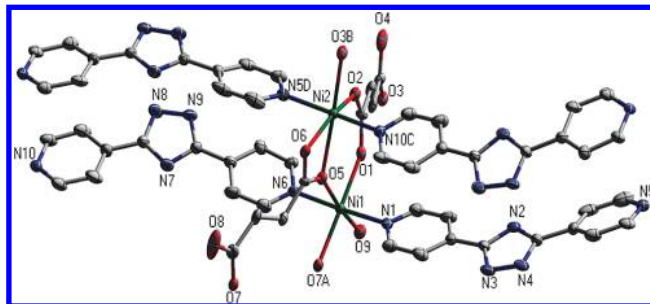


Figure 1. ORTEP view of **1** with thermal ellipsoids at 30% probability showing the coordination environments of the Ni^{II} atoms.

tion corrections were applied by *SADABS*.¹⁷ The structures were solved by direct methods and refined using a full-matrix least-squares technique with *SHELXL-97*.¹⁷ C-bound H atoms were placed geometrically and refined as riding atoms; N-bound H atoms were located in difference Fourier syntheses, and refinement proceeded using a rigid model. With the exception of the solvate H atoms in **1**, which were not located, all other H atoms of the coordinated water in the structures first located on difference Fourier maps and then fixed at calculated positions and were included in the final refinement. Isotropic displacement parameters of all H atoms were derived from the parent atoms. Experimental details of the X-ray analyses are provided in Table 1. Selected bond distances and angles are listed in Table S1 in the Supporting Information.

Results and Discussion

Crystal Structure. As shown in Figure 1, the asymmetric unit of **1** has two crystallographically independent Ni atoms, both displaying slightly distorted octahedral coordination geometries. The Ni1 center is coordinated by four equatorial O atoms from three fum ligands and one coordinated water molecule [Ni1–O = 2.041(4)–2.110(4) Å] and two apical N atoms from two bpt ligands [Ni1–N = 2.079(5)–2.093(5) Å]; Ni2 is coordinated by four equatorial carboxylate O atoms from three fum ligands [Ni2–O = 1.982(4)–2.159(4) Å] and two apical N atoms from two bpt ligands [Ni2–N = 2.073(5)–2.155(5) Å]. The Ni2 atom is linked to Ni1 atoms with mixed bridges through one trans-related carboxyl O atom and one syn–syn carboxylate from the fum group [Ni1···Ni2 = 3.732(8) Å; Ni1–O5–Ni2 = 122.9(2)°] to form a dimeric unit. The adjacent dimeric units

(12) (a) Binder, K.; Young, A. P. *Rev. Mod. Phys.* **1986**, *58*, 801. (b) Taniguchi, T.; Yamanaka, K.; Sumioka, H.; Yamazaki, T.; Tabata, Y.; Kawarazaki, S. *Phys. Rev. Lett.* **2004**, *93*, 246605. (c) Sourlas, N. *Nature* **1989**, *339*, 693.

(13) (a) Belik, A. A.; Takayama-Muromachi, E. *Inorg. Chem.* **2006**, *45*, 10224. (b) Li, D. X.; Nimori, S.; Shiokawa, Y.; Haga, Y.; Yamamoto, E.; Onuki, Y. *Phys. Rev.* **2003**, *B68*, 172405. (c) Cordero, F.; Paoloneb, A.; Cantelli, R.; Magn, J. *Magn. Mater.* **2004**, *272*, 185. (d) Wang, Y.-T.; Bai, H.-Y.; Pan, M.-X.; Zhao, D.-Q.; Wang, W.-H. *Phys. Rev.* **2006**, *B74*, 064422. (e) Jiao, F.; Harrison, A.; Bruce, P. G. *Angew. Chem., Int. Ed.* **2007**, *46*, 3946.

(14) (a) Benelli, C.; Blake, A. J.; Brechin, E. K.; Coles, S. J.; Graham, A.; Harris, S. G.; Meier, S.; Parkin, A.; Parsons, S.; Seddon, A. M.; Winpenny, R. E. P. *Chem.—Eur. J.* **2000**, *6*, 883. (b) Yang, E.-C.; Wernsdorfer, W.; Zakharov, L. N.; Karaki, Y.; Yamaguchi, A.; Isidro, R. M.; Lu, G. D.; Wilson, S. A.; Rheingold, A. L.; Ishimoto, H.; Hendrickson, D. N. *Inorg. Chem.* **2006**, *45*, 529. (c) Bell, A.; Aromi, G.; Teat, S. J.; Wernsdorfer, W.; Winpenny, R. E. P. *Chem. Commun.* **2005**, 2808. (d) Xu, J.-Y.; Qiao, X.; Song, H.-B.; Yan, S.-P.; Liao, D.-Z.; Gao, S.; Journaux, Y.; Cano, J. *Chem. Commun.* **2008**, 6414.

(15) (a) Buschmann, W. E.; Ensling, J.; Gütllich, P.; Miller, J. S. *Chem.—Eur. J.* **1999**, *5*, 3019. (b) Buschmann, W. E.; Miller, J. S. *Inorg. Chem.* **2000**, *39*, 2411. (c) Culp, J. T.; Park, J. H.; Meisel, M. W.; Talham, D. R. *Inorg. Chem.* **2003**, *42*, 2842. (d) Pardo, E.; Burgette, P.; Ruiz-García, R.; Julve, M.; Beltrán, D.; Journaux, Y.; Amorós, P.; Lloret, F. *J. Mater. Chem.* **2006**, *16*, 2702. (e) Kim, J.; Han, S.; Pokhodnya, K. I.; Miglioni, J. M.; Miller, J. S. *Inorg. Chem.* **2005**, *44*, 6983.

(16) Huang, F.-P.; Tian, J.-L.; Li, D.-D.; Chen, G.-J.; Gu, W.; Yan, S.-P.; Liu, X.; Liao, D.-Z.; Cheng, P. *CrystEngComm* **2010**, DOI: 10.1039/B911950G.

(17) (a) Sheldrick, G. M. *SADABS 2.05*; University Göttingen; Göttingen, Germany. (b) *SHELXTL 6.10*; Bruker Analytical Instrumentation: Madison, WI, **2000**.

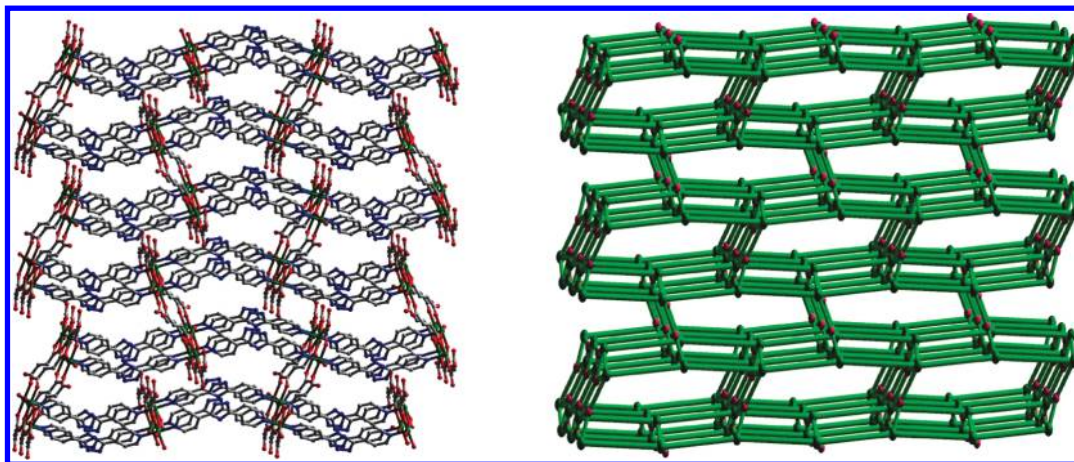


Figure 2. View of (left) the 3D (3,5)-connected “brick-wall”-like architecture of **1** and (right) its schematic description.

are linked by fum to generate a ladderlike chain running along the crystallographic a axis [$\text{Ni}\cdots\text{Ni} = 6.163(1)$, $8.806(1)$, and $8.280(1)$ Å; Figure S1 in the Supporting Information]. The chain is further connected by bpt pillars to generate a noninterpenetrating 3D “brick-wall”-like open framework with a 1D solvent-filled channel (24.3% of the cell volume calculated by *PLATON*¹⁸), as shown in Figure 2 (left), and the interchain $\text{Ni}\cdots\text{Ni}$ distance is $14.216(2)$ Å. Owing to the steric hindrance of the dicarboxylate, entity charge balance, and coordination mode of the metal ion, the fum ligand should find it difficult to form a 3D structure in the absence of bpt.¹⁹ In fact, the appropriate degree of chemical flexibility of subsidiary ligand bpt is probably favorable for a self-filling structure.

Better insight into this framework can be achieved by topology analysis. Considering the coordination modes of fum, which is linked three times to the metal center, it can be viewed as a three-connected node, and the metal atom Ni is viewed as a five-connected node; thus, as seen in Figure 2 (right), a (3,5) topology with the short Schläfli symbol of $(4^2.6)(4^2.6^5.8^3)$ could be observed. To our knowledge, this topology is rarely reported,²⁰ which is different from the other (3,5)-connected nets, for example, the coordination net with $(6^3)(6^9.8)$ topology.²¹ This discovery of this novel topology is useful at the basic level in the crystal engineering of coordination networks.

Magnetic Studies. Magnetic susceptibility measurements carried out on crushed single crystals of **1** with 1 kOe. The $\chi_{\text{M}}T$ value per Ni2 unit at 300 K is $2.41 \text{ cm}^3 \text{ K mol}^{-1}$, which is close to the spin-only value ($2.00 \text{ cm}^3 \text{ K mol}^{-1}$). First, it exhibits a monotonic decrease in $\chi_{\text{M}}T$ until a minimum ($1.19 \text{ cm}^3 \text{ K mol}^{-1}$) at 10 K with decreasing temperature, which indicates a dominant AF interaction between the Ni^{II} ions, and then an increase upon further

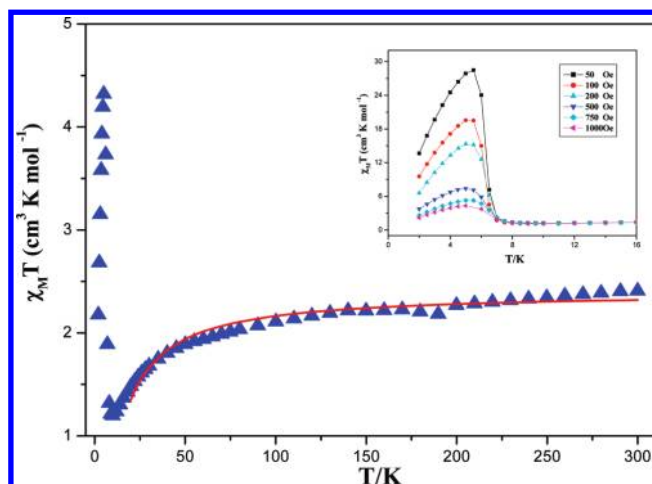


Figure 3. Temperature dependence of magnetic susceptibility of **1**. The line represents the best fit of the data. Inset: FC magnetization.

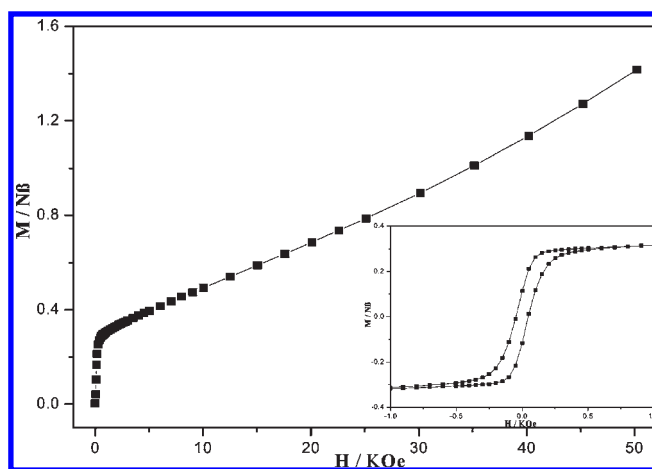


Figure 4. Field-dependent magnetization and hysteresis loop (inset) for **1** at 2 K.

lowering of the temperature, a peak ($4.32 \text{ cm}^3 \text{ K mol}^{-1}$) at 5 K, and finally a rapid decrease to a value of $2.18 \text{ cm}^3 \text{ K mol}^{-1}$ at 2 K (Figure 3), indicating an AF-like behavior or a system of spin canting followed by the effect of the D parameter (or saturation phenomena). Because the shortest $\text{Ni}\cdots\text{Ni}$ distance across the bpt or fum bridge is

(18) Spek, A. L. *PLATON, A multipurpose Crystallographic Tool*; Utrecht University: Utrecht, The Netherlands, 2001.

(19) (a) Ma, B.-Q.; Mulfort, K. L.; Hupp, J. T. *Inorg. Chem.* **2005**, *44*, 4912. (b) Michaelides, A.; Skoulika, S.; Siskos, M. G. *Chem. Commun.* **2004**, 2418. (c) Zhang, K.-L.; Liang, W.-L.; Chang, Y.; Ng, S. W. *Polyhedron* **2009**, *28*, 647.

(20) Gilmore, C. J.; Speakman, J. C. *Acta Crystallogr., Sect. B* **1982**, *38*, 2809.

(21) (a) Abrahams, B. F.; Batten, S. R.; Hoskins, B. F.; Robson, R. *Inorg. Chem.* **2003**, *42*, 2654. (b) Carlucci, L.; Ciani, G.; Proserpio, D. M.; Rizzato, S. *CrystEngComm* **2002**, *4*, 413. (c) Fan, J.; Zhu, H.-F.; Okamura, T.; Sun, W.-Y.; Tang, W.-X.; Ueyama, N. *Chem.—Eur. J.* **2003**, *9*, 4724.

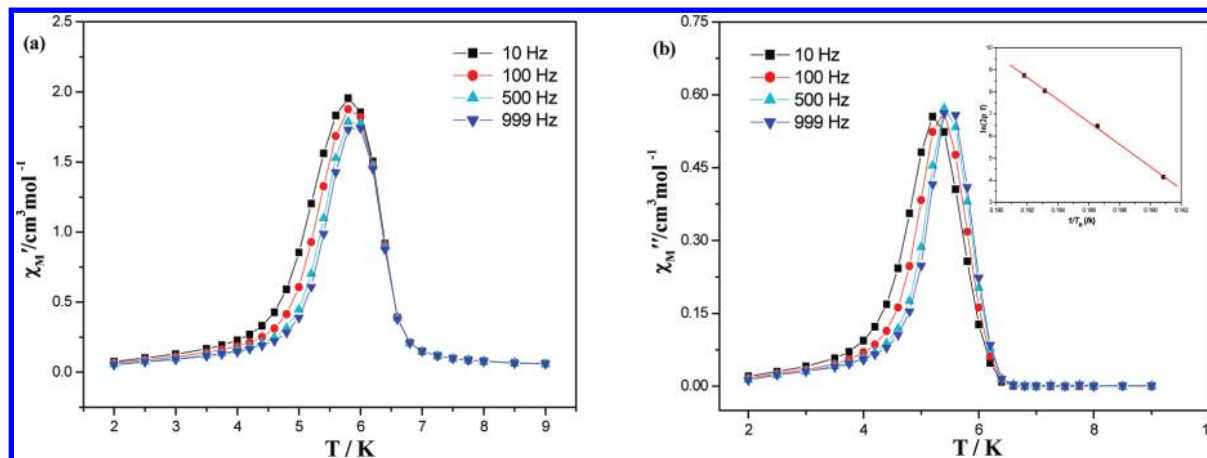


Figure 5. Temperature dependence of the in-phase (a) and out-of-phase (b) ac magnetic susceptibilities for **1**. (b, inset) Linear fit of the experimental data to the Arrhenius law.

6.163(1) Å in **1**, the magnetic exchange coupling through these bridges is expected to be very weak. The observed dominant AF interaction should mainly arise from the magnetic superexchange through the carboxylato and oxo bridges in the Ni₂ dimeric subunit. To understand the high-temperature behavior, we used the known expression given by Kahn²² to fit the experimental data from 300 to 10 K. We have applied the mean-field approach to calculate the intermolecular interactions (zJ'). The best-fit parameters to reproduce satisfactorily the experimental data are $g = 2.19$, $J = -4.13 \text{ cm}^{-1}$, and $zJ' = -0.51 \text{ cm}^{-1}$. However, it should be noted that the results only imply weak AF exchanges between metal ions in **1**, while an exact estimation of the magnetic interactions is unattainable because of the single-ion anisotropy (D parameter) in these Ni^{II} systems.

To further investigate the phase transformation at low temperature, the field-cooled (FC) and zero-field-cooled (ZFC) magnetization measurements were performed at 50 Oe in the 2–20 K range (Figure S2 in the Supporting Information). Below 7 K, the FC curve of **1** shows an abrupt increase with decreasing temperature, reaching saturation at lower T values, while the ZFC curve exhibits a rounded maximum and falls below $T = 5$ K. The FC and ZFC data are divergent below the critical temperature $T_c = 5$ K, suggesting a long-range FO phase transition below this temperature.²³ Moreover, FC magnetizations were measured under different applied fields. The magnetic behaviors are quite field-dependent, in which the increases of the $\chi_M T$ values at low temperature become less pronounced at higher fields (Figure 3, inset). This is an important feature of spin-canting behavior.²⁴ The FO transition is further confirmed by the field-dependent isothermal magnetization $M(H)$ performed at 2 K. As shown in Figure 4, an abrupt increase of magnetization to a value of ca. $0.29 N\mu_B$ is observed at

0.6 kOe. When the external field is further increased, the magnetization shows a slow increase and approaches a value of $1.42 N\mu_B$ at 50 kOe, which is far below the saturation value of $4.4 N\mu_B$ expected for the Ni₂ unit ($S = 1$; $g = 2.2$), indicating the occurrence of canted antiferromagnetism. The magnetic hysteresis loop is observed at 2 K, with the coercive field (H_c) and the remnant magnetization (M_R) being 50.4 Oe and $0.283 N\mu_B$, respectively, indicating a soft-magnetic behavior of **1** (Figure 4, inset). The canting angle can be estimated through the equation²² $\sin(\gamma) = M_R/M_S$ ($M_S = gSN\mu_B = 4.4 N\mu_B$) to be up to 3.7° .

The zero-field alternating-current (ac) magnetic susceptibility measurements were performed under $H_{ac} = 5$ Oe and a frequency of 10–999 Hz (Figure 5). Surprisingly, both of the in-phase and out-of-phase signals, χ_M' and χ_M'' , display a small but nonnegligible frequency-dependent behavior, which suggests a slow relaxation process characteristic of a SG transition.²⁵ The frequency-dependent normalized frequency shift in the freezing temperature, T_f , of the peak temperature shift (ΔT_p) of χ_M' , as measured by the parameter $\phi = \Delta T_p/[T_p \Delta(\log f)] = 0.0086$ (f is the frequency of H_{ac}), is consistent with a cluster glasslike magnetic behavior. Generally speaking, the ϕ value is larger than 0.1 for a SMM, while it is usually smaller than 0.01 for a typical SG.^{25a} The relaxation time τ , which was extracted from the maximum of χ_M'' at different frequencies, follows an Arrhenius law dependence, $\tau(T_f) = \tau_0 \exp(\Delta/k_B T_f)$, where τ_0 , Δ , and k_B are the preexponential factor, the relaxation energy barrier, and the Boltzmann constant, respectively. The least-squares fitting of the experimental data of **1** to the Arrhenius law typically gives values of $\tau_0 = 1.4 \times 10^{-43}$ s and $\Delta/k_B = 507$ K. The big Δ/k_B value suggests that the movement of the domain walls is difficult;²⁶ thus, we further conclude that the slow relaxation behavior comes from the SG state because **1** presents simultaneous FO (from the spin canting) and AF (from the –O– and

(22) Kahn, O. *Molecular Magnetism*; VCH: New York, 1993.

(23) Chernova, N. A.; Song, Y.-N.; Zavalij, P. Y.; Whittingham, M. S. *Phys. Rev. B* **2004**, *70*, 144405.

(24) (a) Wang, X.-Y.; Wei, H.-Y.; Wang, Z.-M.; Chen, Z.-D.; Gao, S. *Inorg. Chem.* **2005**, *44*, 572. (b) Brechin, E. K.; Cador, O.; Caneschi, A.; Cadiou, C.; Harris, S. G.; Parsons, S.; Vonci, M.; Winpenny, R. E. P. *Chem. Commun.* **2002**, 1860. (c) Escuer, A.; Cano, J.; Goher, M. A. S.; Journaux, Y.; Lloret, F.; Mautner, F. A.; Vicente, R. *Inorg. Chem.* **2000**, *39*, 4688. (d) Cheng, X.-N.; Xue, W.; Zhang, W.-X.; Chen, X.-M. *Chem. Mater.* **2008**, *20*, 5345.

(25) (a) Mydosh, J. A. *Spin Glasses*; Taylor and Francis: Washington, DC, 1993. (b) O'Connor, C. J. *Research Frontiers in Magnetochemistry*; World Scientific: River Edge, NJ, 1993.

(26) (a) Bellouard, F.; Clemente-León, M.; Coronado, E.; Galán-Mascarós, J. R.; Gómez-García, C. J.; Romero, F.; Dunbar, K. R. *Eur. J. Inorg. Chem.* **2002**, 1603. (b) Coronado, E.; Gómez-García, C. J.; Nuez, A.; Romero, F. M.; Rusanov, E.; Stoeckli-Evans, H. *Inorg. Chem.* **2002**, *41*, 4615.

–OCO– bridges) exchange couplings and may present some degree of frustration in the very complex magnetic lattice.^{25a,27} Apparently, complex **1** shows quite unusual magnetic behavior and is tentatively ascribed to the canted antiferromagnet with SG relaxation. Finally, the needed randomness in the magnetic lattice may arise from crystal defects and/or from the presence of up to two different coordination environments in the Ni^{II} ions.^{25a}

Conclusions

In summary, we report here a pillared “brick-wall”-like 3D nickel–organic framework formulated as $\{[\text{Ni}_2(\text{fum})_2(\text{bpt})_2(\text{H}_2\text{O})] \cdot 3\text{H}_2\text{O}\}_n$ (**1**) with promising structural features and properties. As far as we know, this is the first example of a nickel carboxylate that exhibits the coexistence of weak ferromagnetism and relaxation behavior. Furthermore, these results

(27) Simon, M. H.; Antonio, A.; Carlos, J. G. G.; Paul, T. W. *Chem. Commun.* **2006**, 1607.

strongly justify further work on the above mixed carboxylate systems with long pillared coligands and other transition metals may lead to even more interesting pillared frameworks.

Acknowledgment. This work was supported by the National Natural Science Foundation of China (Grants 20771063 and 90922032).

Supporting Information Available: Crystallographic data (CIF), graphics showing coordination modes, tables for pertinent bonding parameters of **1**, and additional information about physical characterizations. This material is available free of charge via the Internet at <http://pubs.acs.org>. CCDC reference number 751825 for compound **1** contains the supplementary crystallographic data for this paper. These data can be obtained free of charge via www.ccdc.cam.ac.uk/conts/retrieving.html (or from the Cambridge Crystallographic Centre, 12 Union Road, Cambridge CB21EZ, U.K.; fax (+44)1223-336-033 or e-mail deposit@ccdc.cam.ac.uk).